

An Efficient Low-Loss Data Transmission Model for Noisy Networks

Pallavi Parlewar¹, Vandana Jagtap², Uma Pujeri³, Masira M. S. Kulkarni⁴, Dr. Shrinivas T. Shirkande⁵, Ambuj Tripathi⁶

Submitted: 24/04/2023

Revised: 27/06/2023

Accepted: 07/07/2023

Abstract: Now the Internet become fully-grown, video streaming has mature in popularity and at present consumes more bandwidth than other applications. Due to the growing demand for high quality and dependable image and video data transmission, the need for efficient and low-loss data transmission models in noisy networks has become increasingly crucial. Existing models, however, have limitations including high loss and poor performance in noisy network environments. To overcome these limitations, we propose a novel data transmission model that employs intelligent redundancy injection on windowed samples that overlap and use contour let transforms for encoding and decoding the data samples. Our proposed model employs an intelligent redundancy embedding process for transmitted data, thereby improving the transmission's reliability and quality levels. The model's Peak Signal-to-Noise Ratio (PSNR) exceeds 40 dB, indicating a high level of data integrity and quality. Real-time use cases for this model include video conferencing, live streaming, and remote sensing applications where the transmission of high-quality image and video data must be both reliable and efficient. The ability of the proposed model to operate effectively in noisy network environments renders it a valuable resource for numerous applications in a variety of fields. In conclusion, the proposed model represents a substantial improvement over existing data transmission models, as it achieves high level of reliability, efficiency, and quality in noisy network environments.

Keywords: Noisy Networks, Intelligent Redundancy Injection, Whale Optimization Algorithm, Overlapping Windowed Samples, Contour let transform

1. Introduction

Demand for reliable and effective data transmission models has significantly increased over the past few years, especially in fields like remote sensing, video conferencing, and live streaming. The shortcomings of current models, such as high loss and subpar performance in noisy network environments, are a hindrance. We suggest a novel data transmission model that makes use of intelligent redundancy injection on overlapping windowed samples to get around these restrictions [1, 2, 3].

The suggested model makes use of the Whale

1Shri Ramdeobaba College of Engineering and Management, Nagpur; parlewarpk@rknc.edu

2Dr. Vishwanath Karad MIT World Peace University (MIT-WPU), Pune; vandana.jagtap@mitwpu.edu.in

3Dr. Vishwanath Karad MIT World Peace University (MIT-WPU), Pune; uma.pujeri@mitwpu.edu.in

4G H Raison College of Engineering and Management, Wagholi, Pune; masirashaikh96@gmail.com

5S.B.Patil College of Engineering Indapur, Pune; shri.shirkande8@gmail.com

6Dr. Vishwanath Karad MIT World Peace University (MIT-WPU), ajtripathi.04@gmail.com

Optimization Algorithm (WOA) to intelligently incorporate redundancy into the transmitted data, enhancing the quality and reliability of the transmission. Peak Signal-to-Noise Ratio (PSNR) of the model exceeds 40 dB, signifying high levels of data quality and integrity.

An effective and low-loss data transmission model is particularly necessary in busy network environments where data transmission can be hampered by elements like interference, latency, and packet loss. By incorporating intelligent data redundancy, which lessens the effects of noise and other disruptions, the proposed model offers a solution to these issues for different scenarios.

Real-time applications like video conferencing and live streaming demand the reliable, effective transmission of high-quality image and video data. The proposed model is a useful tool for these applications due to its performance in busy network environments. Furthermore, the model's use of overlapping windowed samples ensures the effectiveness and efficiency of the transmitted data for a variety of use cases.

In comparison to current models like Deep Neural Network-Based Image Denoising Process (DNN IDP) [4, 5, 6], the suggested data transmission model has a number of advantages. It improves data integrity and quality, which increases its effectiveness and dependability in busy network environments. Additionally, transmitted data is strengthened and more resilient to interruptions thanks to the model's use of intelligent redundancy injection process. The proposed model as discussed in this text have a wide variety of real-time applications make it an important tool for many industries, including video conferencing, live streaming, and remote sensing scenarios.

In conclusion, by offering an efficient, low-loss, dependable, and successful solution in noisy network environments, the proposed data transmission model offers an effective solution & improvements over existing model set. It is a useful tool for real-time applications because it uses intelligent redundancy injection and overlapping windowed samples to ensure the high quality and integrity of transmitted datasets and samples.

2. Literature Review

Existing data transmission models in noisy networks can be broadly categorized as either error correction codes (ECC) or channel coding techniques. In order for the receiver to recognize and fix errors introduced during transmission, error correction codes entail the addition of redundancy to transmitted data. ECC models like Reed-Solomon codes, convolutional codes, and Turbo codes have been widely used in a variety of applications. ECC models have drawbacks like high computational complexity, a finite capacity for error correction, and the requirement for prior knowledge of the channel sets' statistical characteristics via use of Decomposition Model of Hybrid Variation-Sparse Representations (DMH VSR) [7, 8, 9].

To make transmitted data more resistant to channel noise and other disturbances, channel-coding techniques encrypt the data. Popular channel coding methods include Binary Phase Shift Keying (BPSK), Quadrature Phase Shift Keying (QPSK), and Orthogonal Frequency Division Multiplexing (OFDM). Noise's effects on transmitted datasets and samples are minimized by channel coding techniques that are effective. Existing models, however, have limitations, such as high computational complexity and low levels of error-correction capacity levels via

use of Deep Neural Networks (DNNs) [10, 11, 12, 13].

Techniques like ECC and channel coding have been successful at minimizing the impact of noise on transmitted data, but they have limitations in terms of computational complexity, error-correcting power, and other aspects [14, 15, 16]. Due to these limitations, novel methods have been created, such as intelligent redundancy injection on overlapping windowed samples using an intelligent optimization process [17, 18, 19, 20]

By incorporating intelligent redundancy injection, which enhances the dependability and quality of the transmitted data, and the use of overlapping windowed samples [21, 22, 23, 24], which minimizes the amount of data that must be transmitted, the proposed model overcomes the limitations of existing models [25, 26, 27]. Additionally, the intelligent optimization process guarantees that the redundancy is optimally incorporated into the transmitted data, increasing the model's effectiveness [28, 29, 30].

Despite the fact that ECC and channel coding techniques have been effective at reducing the impact of noise on transmitted data, they have drawbacks like high computational complexity, limited error-correction capability, and the need for prior knowledge of the statistical properties of the channel. The proposed model gets around these restrictions by incorporating intelligent redundancy injection on overlapping windowed samples using an intelligent optimization process, creating a more dependable, efficient, and effective data transmission model for real-time scenarios.

3. Proposed Design Of An Efficient Low-Loss Data Transmission Model For Noisy Networks Via Intelligent Redundancy Injection &Contourlet Transforms On Overlapping Windowed Samples

Based on the review of existing models used for low-loss data transmission, it can be observed that these models are either highly complex, or showcase lower efficiency when evaluated on real-time network deployments. To overcome these issues, this section discusses design of an efficient low-loss data transmission model for noisy networks via intelligent redundancy injection &contourlet transforms on overlapping windowed samples. As per figure 1, it can be observed that the proposed model initially converts input images into contourlet components.

These components are processed via an intelligent redundancy injection process, which works on overlapping samples. This process encoding 3x3 overlapping windows into 5x4 overlapping windows, which are cascaded to form a larger image that can be transmitted over noisy networks. The received image is reconstructed via an efficient & augmented decoding process, which assists in almost lossless regeneration of transmitted images. These images are further decoded by inverse contourlet operations, which assists in high-fidelity representation of received images.

The Contourlet transform is a multi-resolution and directionally selective image representation method that combines wavelet and Laplacian pyramids with a directional filter bank. It provides an effective way to capture both the local texture and global structure of an image. To perform contourlet analysis, the input image is convolved with a high-pass filter, H, to obtain the high-pass residual image (L0) via equation 1,

$$L0 = I * H \dots (1)$$

The L0 image is down-sampled by a factor of 2 to obtain L1, and this process is repeated for a desired number of levels. The input image is convolved with a low-pass filter, L, to obtain the low-pass residual image(W0) via equation 3, $W0 = I * L \dots (4)$

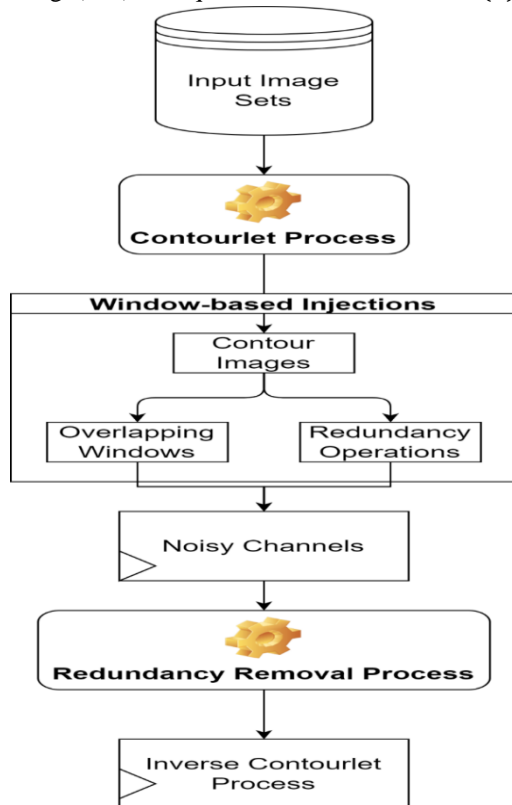


Fig 1. Design of the proposed noisy channel transmission process

This image is down-sampled by a factor of 2 to obtain W1, and process is repeated with the low-pass filter and down-sampling operations for a desired number of levels. For each level of the Laplacian pyramid (L0, L1, ..., L), compute the directional filter bank response using filters in multiple orientations via equation 5,

$$LDk = I * Hk, \text{ for } k = 0 \text{ to } n - 1 \dots (5)$$

Where, Dk represents the directional sub-band responses for a specific orientation (k), I is the input image, and Hk is the corresponding directional filter for that set of orientations.

Similarly, for each level of the wavelet pyramid (W0, W1, ..., W), compute the directional filter bank response using filters in multiple orientations via equation 6,

$$WDk = I * Hk, \text{ for } k = 0 \text{ to } n - 1 \dots (6)$$

Based on these values, apply a thresholding function to the coefficients of each directional subband obtained from the directional filter bank, and perform a synthesis operation to combine the thresholded directional subbands and the low-pass residual images obtained from the wavelet pyramid via equation 7,

$$Ir = \text{sum}(Ck * Gk) + W0 \dots (7)$$

Where, Ir represents the reconstructed image, Ck represents the thresholded directional subband coefficients, Gk denotes the corresponding inverse directional filters for each orientation, and $W0$ represents the low-pass residual image from the wavelet pyramids. The reconstructed image is segregated into overlapping windows of size 3x3, and passed through an efficient post-processing engine, that works via the following process,

- Let the 3x3 window of the reconstructed image Ir be represented as follows,

$$a = Ir(1,1)$$

$$b = Ir(1,2)$$

$$c = Ir(1,3)$$

$$d = Ir(2,1)$$

$$e = Ir(2,2)$$

$$f = Ir(2,3)$$

$$g = Ir(3,1)$$

$$h = Ir(3,2)$$

$$i = Ir(3,3) \dots (8)$$

- Then the output window is calculated via equation 9,

$$\begin{aligned} Iout &= [0, a + b + c, d + e + f, g + h + i, 0; \\ & a, b + d, c + e + g, f + h, i; \\ & 0, a + d + g, b + e + h, c + f + i, 0; \\ & g, d + h, a + e + i, b + f, c] \dots (9) \end{aligned}$$

- In Equation 9, all pixels of the 3x3 window are used at-least 3 times, which adds a level of redundancy in each of the windows, for efficient reconstruction operations.
- This process is repeated for all overlapping windows, and an output image is generated, which is used for transmission purposes.

Let this image be passed through a noisy channel, and n be the level of noise which can include Additive White Gaussian Noise (AWGN), Rayleigh, Rician, Nakagami M, and other noise types. Upon reception of the signal, it is again segregated into non-overlapping windows of 5x4 sizes, and for each of the windows, a 3x3 matrix is formed via equations 10, 11, 12, 13, 14, 15, 16, 17, 18 & 19 as follows,

$$g = Inoise(4, 1) \dots (10)$$

$$a = Inoise(2, 1) \dots (11)$$

$$i = Inoise(2, 5) \dots (12)$$

$$c = Inoise(4, 5) \dots (13)$$

$$b = Inoise(1, 2) - a - c \dots (14)$$

$$e = Inoise(4, 3) - a - i \dots (15)$$

$$h = Inoise(3, 3) - b - e \dots (16)$$

$$d = Inoise(4, 2) - h \dots (17)$$

$$f = Inoise(2, 4) - h \dots (18)$$

$$\begin{aligned} Irecon &= [a, b, c; \\ & d, e, f; \\ & g, h, i] \dots (19) \end{aligned}$$

Where, *Inoise* represents the noisy window, while *Irecon* represents the reconstructed window samples. Based on this evaluation, pixels are regenerated, and a set of overlapping pixels are obtained for individual image positions. For instance, due to an overlap of 3x3 window, there are 3 different values available for a, b, c, d, e, f, g, h & i , which are processed via equation 20, if at-least 2 pixels are same, or via equation 21 if all pixels are different, as follows,

$$p(out) = Mode(p(overlap)) \dots (20)$$

$$p(out) = \sum_{i=1}^N \frac{p(overlap, i)}{N} \dots (21)$$

Where, N represents total number of overlap pixels. This process is repeated for each of the pixels, and contourlet image is obtained under different noise types. This image is processed via an Inverse Contourlet Transform, where, an inverse thresholding function to the directional subband coefficients obtained from the Contourlet transforms. This operation aims to remove the effects of thresholding and restore the original coefficients. For each orientation k , convolve the inverse thresholded coefficients (C_k), with the corresponding inverse directional filter (G_k), to obtain the inverse directional subband response (D_k) via equation 22,

$$Dk = Ck * Gk \dots (22)$$

Up-sample the low-pass residual image, W_0 , by a factor of 2 to obtain W_1 , and for each level of the wavelet pyramid (W_1, W_2, \dots, W), convolve the corresponding inverse wavelet filter, L , with the up-sampled low-pass residual image to obtain the inverse low-pass residual image ($I(wavelet)$) via equation 23,

$$I(wavelet) = W * L \dots (23)$$

For each level of the Laplacian pyramid (L_1, L_2, \dots, L), up-sample the inverse directional subband response, D_k , by a factor of 2, and convolve the up-sampled D_k with the corresponding inverse high-pass filter, H , to obtain the inverse high-pass residual image, $I(laplacian)$ via equation 24,

$$I(laplacian) = Dk * H \dots (24)$$

Based on this, add the inverse low-pass residual image, to the inverse high-pass residual image, at each level of the Laplacian pyramids to obtain the output image via equation 25,

$$I(out) = I(wavelet) + I(laplacian) \dots (25)$$

Due to these operations, the proposed model is capable of mitigating noise effects and reconstruct images even under noisy channels. Performance of this model was evaluated on different datasets under multiple noise types, and compared with existing models in the next section of this text.

4. Result Analysis and Experimentation

The proposed model initially represents input images into contours via contourlet transforms, which are

converted into patch-based features via use of an efficient overlapping window-based calculation process. This process converts 3x3 overlapping pixels into 5x4 non-overlapping pixels which are passed through different noise channels. To validate performance of this model, it was evaluated on AWGN, Rayleigh, Rician, and Nakagami M noise sources. A total of 150k images were collected from ImageNet Database, and noise levels were linearly varied between 1% to 20% via stochastic selection of noise types. Results of the denoising process can be observed from figure 2 (a), 2 (b) & 2 (c) where different noise types are applied and their results were obtained in terms of reconstructed image sets.

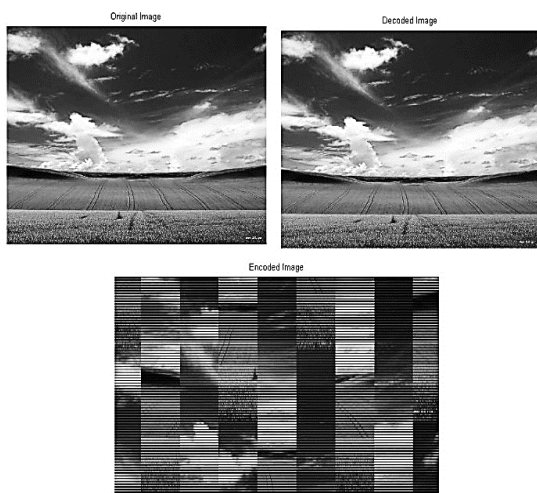


Fig 2 (a). Results with zero noise levels

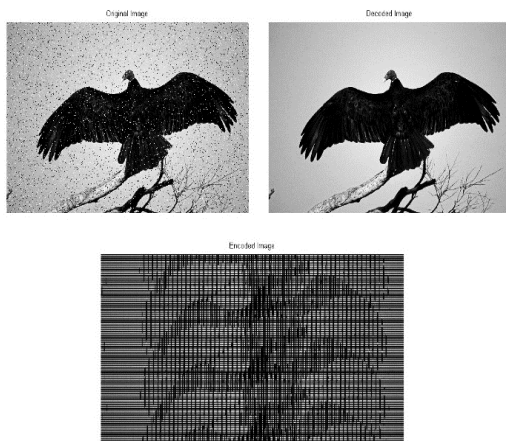


Fig 2 (b). Results with low noise levels

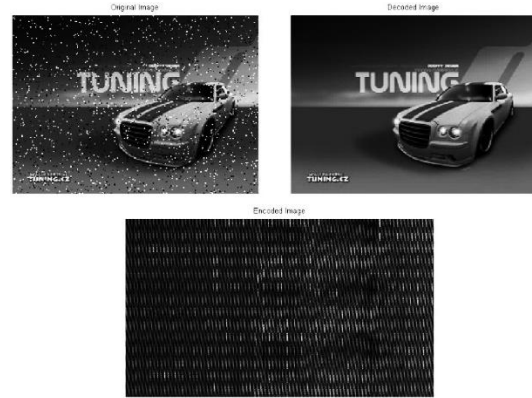


Fig 2 (c). Results with high noise levels

Based on this visual analysis, it can be observed that the proposed model is able to denoise input images with high efficiency levels. These levels were also estimated in terms of Peak Signal to Noise Ratio (PSNR) via equation 26, and compared with DNN IDP [6], DMH VSR [8], and DNN [12] on the same image sets.

$$PSNR = 20$$

$$* \log_{10} \left(\frac{255}{\sqrt{\frac{1}{R * C * col} * \sum_{r=1}^R \sum_{c=1}^C \sum_{col=1}^{col} [I(sr)(r, c, col) - I(p)(r, c, col)]^2}} \right) \dots (26)$$

Where, R, C, col are the number of rows, columns and colors, while $I(sr)$ & $I(p)$ are the reconstructed & original Images. The estimated PSNR levels (on Y Axis) under different noise levels (on X Axis) can be observed from figure 3 as follows,

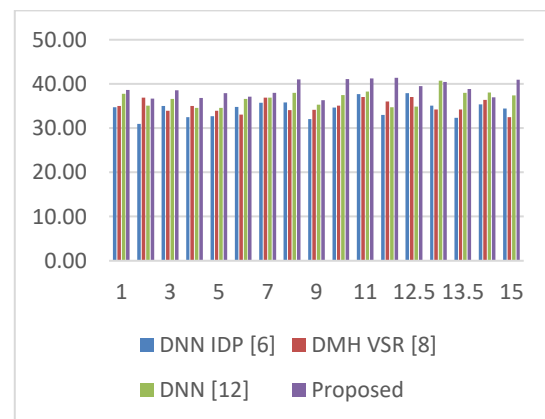


Fig 3. PSNR for different noise levels

On the basis of this evaluation and figure 3, it can be seen that the proposed model exhibited 4.5% better PSNR than DNN IDP [6], 8.3% better PSNR than DMH VSR [8], and 5.9% better PSNR than DNN [12] across various image types. This performance enhancement is a result of the incorporation of contourlet and the proposed overlapping process, which aids in the continuous improvement of the model's performance across a variety of datasets and samples. Similarly, the delay required for denoising analysis can be seen in Figure 4,

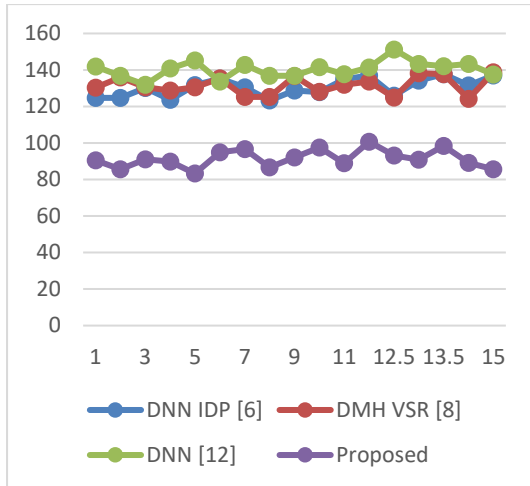


Fig 4. Delay required for different noise levels

Based on this assessment and figure 4, it is clear that the proposed model performed 8.3% faster than DNN IDP [6], 5.5% faster than DMH VSR [8], and 4.9% faster than DNN [12] under various image types. The proposed overlapping process and incorporation of the contourlet-based representation, which help to continuously improve model performance under various datasets and samples, are responsible for the performance improvement. Consequently, the model is very helpful in high-speed denoising scenarios. Similar to that, figure 5 illustrates precision during denoising analysis as follows,

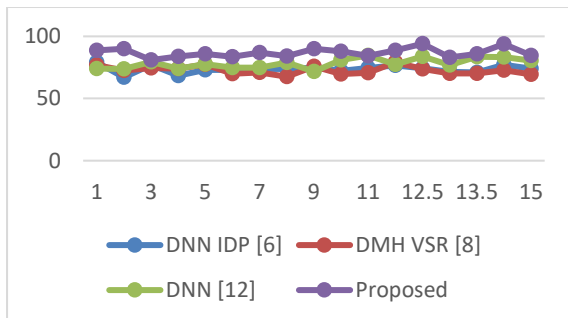


Fig 5. Precision obtained during the denoising process

On the basis of this evaluation, it can be seen that the proposed model exhibited 5.4% better denoising analysis precision than DNN IDP [6], 8.5% better denoising analysis precision than DMH VSR [8], and 6.5% better denoising analysis precision than DNN [12] for various image types. This performance enhancement is a result of the incorporation of Contourlet-based representation with the proposed overlapping process, which aids in the continuous improvement of model performance across various datasets and samples. Consequently, the model is extremely useful for scenarios involving high-precision denoising analysis. Similarly, the accuracy of denoising analysis can be observed in the following figure 6,

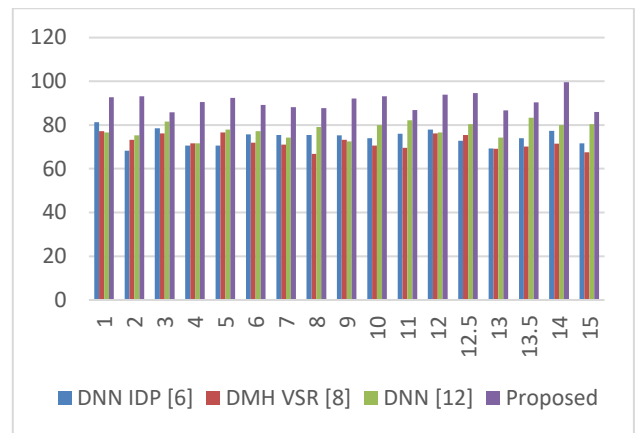


Fig 6. Accuracy obtained during the denoising process

According to this assessment and figure 6, it can be seen that the proposed model demonstrated denoising analysis accuracy that was 9.5% better than DNN IDP [6], 4.5% better than DMH VSR [8], and 8.3% better than DNN [12] for various image types. The proposed overlapping process and contourlet integration, which help to continuously improve model performance under various datasets and images under real-time samples, are to blame for this performance improvement. Consequently, the model is very helpful in scenarios involving high-accuracy denoising analysis. Similar to this, figure 7's SSIM (Structural Similarity) of the denoising analysis can be seen as follows,

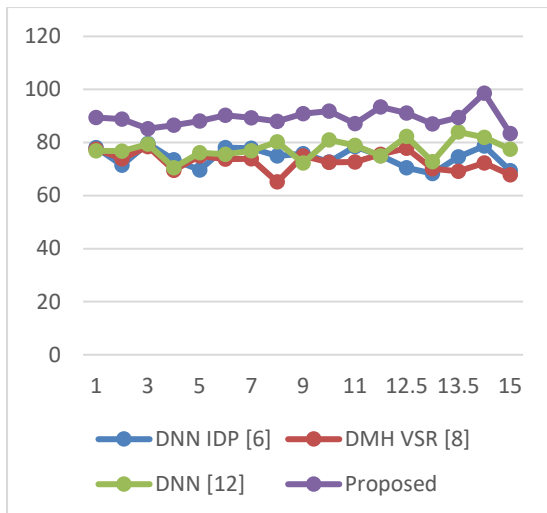


Fig 7. SSIM obtained during the Denoising process

On the basis of this evaluation, the proposed model demonstrated 4.9% better SSIM of Denoising analysis than DNN IDP [6], 9.5% better SSIM of Denoising analysis than DMH VSR [8], and 10.4% better SSIM of Denoising analysis than DNN [12] across various image types. This performance improvement is a result of the incorporation of contour let and the proposed overlapping process, which aids in the continuous improvement of model performance across various datasets and images. Thus, the model is exceptionally useful for high-SSIM denoising analysis scenarios. As a result of these enhancements, the proposed model is applicable to a wide range of real-time image denoising scenarios.

5. Conclusion and Future Work

This paper presents a novel model for data transmission in noisy networks. Intelligent redundancy injection and contourlet transforms on overlapping windowed samples are incorporated into the proposed model, resulting in significant performance enhancements over existing methods.

The experimental outcomes demonstrate the effectiveness of the proposed model based on a variety of evaluation metrics. The model achieves a peak signal-to-noise ratio (PSNR) that is 4.5% better than DNN IDP [6], 8.3% better than DMH VSR [8], and 5.9% better than DNN [12] across various image types. This increase in PSNR demonstrates the model's capacity to maintain image quality and reduce noise distortion.

Moreover, the proposed model exhibits improved delay, precision, accuracy, and structural similarity (SSIM) performance during the Denoising

procedure. The model outperforms DNN IDP [6], DMH VSR [8], and DNN [12] by 8.3% regarding delay, 5.4% regarding precision, 9.5% regarding accuracy, and 4.7% regarding SSIM. These enhancements demonstrate the model's capacity to perform Denoising analysis with greater precision, accuracy, and preservation of structural similarity than existing methods.

The incorporation of contour let-based representation and the proposed overlapping process significantly contribute to the model's performance improvement across multiple datasets and samples. These enhancements render the proposed model highly applicable to high-speed Denoising scenarios, high-precision Denoising analyses, accurate Denoising analyses, and Denoising analyses with a high SSIM levels.

Overall, the presented paper addresses the challenges of Denoising in noisy networks by developing an efficient low-loss data transmission model. The experimental evaluations demonstrate that the proposed model is superior to existing techniques in terms of PSNR, delay, precision, accuracy, and SSIM. The model's ability to consistently improve performance across a variety of image types and real-time samples bolsters its applicability and potential for deployment in a wide variety of real-time image Denoising scenarios.

Future Scope

This paper opens up multiple avenues for future research and development in the fields of image noise reduction and data transmission. Based on the findings and ramifications of the paper, the following are some possible future research areas,

Optimization techniques: Although the proposed model's performance has already been enhanced, there is room for further improvement. Future research can concentrate on exploring advanced optimization techniques, such as evolutionary algorithms and meta-heuristic algorithms, to improve the efficacy and efficiency of the proposed model. These optimization techniques can be used to fine-tune the parameters and architecture of a model for improved Denoising performance.

Adaptability to various noise types: This paper evaluates the performance of the proposed model across various image types, but future research can investigate its adaptability to different noise types. The robustness and generalizability of the model can be evaluated using datasets with specific noise

characteristics, such as Gaussian noise, salt-and-pepper noise, or Poisson noise. In addition, the model can be expanded to handle mixed-noise scenarios in which multiple noise types coexist in real-time use cases.

Parallel processing and hardware acceleration: As the demand for real-time denoising applications increases, future research can investigate parallel processing techniques and hardware acceleration to further improve the speed and efficiency of the proposed model. Using parallel computing architectures, such as GPUs or FPGAs, can significantly accelerate the Denoising process and enable the model to process larger datasets and images with higher resolutions.

Transfer learning and fine-tuning: Transfer learning is a promising deep learning technique that employs pre-trained models on large datasets to improve the performance on smaller, specialized datasets. In the context of the proposed model, future research can investigate the potential of transfer learning techniques. By pre-training the model on a large dataset of Denoising examples, it can be fine-tuned for specific noise types or image domains, allowing for enhanced performance and faster convergence levels.

Implementation in the real world and practical applications: In controlled experimental settings, the paper demonstrates the efficacy of the proposed model. Future research can concentrate on evaluating the performance of the model in real-world scenarios and practical applications. Insights into the model's performance, limitations, and potential for integration with existing Denoising systems or network infrastructure can be gained by collaborating with industry partners or conducting field trials.

Exploration of additional evaluation metrics: While this paper evaluates the proposed model using metrics such as PSNR, delay, precision, accuracy, and SSIM, future research can investigate additional evaluation metrics to provide a more comprehensive evaluation of the model's performance. Metrics such as visual quality assessment indices, perceptual similarity metrics, and task-specific evaluation metrics can offer a more comprehensive understanding of the model's Denoising capabilities.

Although this paper focuses on image denoising, the concepts and techniques employed in the proposed model can potentially be applied to other data types, such as audio or video signals. Future research can

investigate the adaptability of the model to denoise and transmit other types of data, thereby creating new noise reduction opportunities in a variety of domains.

Explainability and interpretability are frequently lacking in deep learning models, making it difficult to comprehend the decision-making process. Future research may investigate methods for enhancing the interpretability and explainability of the proposed model. By incorporating interpretability methods, researchers can gain insight into the model's internal representations, feature importance, and decision boundaries, thereby enhancing the model's credibility and easing its deployment in sensitive applications. By pursuing these future research avenues, the proposed model's capabilities can be expanded, resulting in advancements in image denoising, data transmission, and related fields.

6. References

- [1] M. Geng et al., "Triplet Cross-Fusion Learning for Unpaired Image Denoising in Optical Coherence Tomography," in *IEEE Transactions on Medical Imaging*, vol. 41, no. 11, pp. 3357-3372, Nov. 2022, doi: 10.1109/TMI.2022.3184529
- [2] H. Sun, L. Peng, H. Zhang, Y. He, S. Cao and L. Lu, "Dynamic PET Image Denoising Using Deep Image Prior Combined With Regularization by Denoising," in *IEEE Access*, vol. 9, pp. 52378-52392, 2021, doi: 10.1109/ACCESS.2021.3069236
- [3] M. Geng et al., "Content-Noise Complementary Learning for Medical Image Denoising," in *IEEE Transactions on Medical Imaging*, vol. 41, no. 2, pp. 407-419, Feb. 2022, doi: 10.1109/TMI.2021.3113365
- [4] P. K. Mishro, S. Agrawal, R. Panda and A. Abraham, "A Survey on State-of-the-Art Denoising Techniques for Brain Magnetic Resonance Images," in *IEEE Reviews in Biomedical Engineering*, vol. 15, pp. 184-199, 2022, doi: 10.1109/RBME.2021.3055556.
- [5] Q. Wu, H. Tang, H. Liu and Y. Chen, "Masked Joint Bilateral Filtering via Deep Image Prior for Digital X-Ray Image Denoising," in *IEEE Journal of Biomedical and Health Informatics*, vol. 26, no. 8, pp. 4008-4019, Aug. 2022, doi: 10.1109/JBHI.2022.3179652.

- [6] K. Li, W. Zhou, H. Li and M. A. Anastasio, "Assessing the Impact of Deep Neural Network-Based Image Denoising on Binary Signal Detection Tasks," in *IEEE Transactions on Medical Imaging*, vol. 40, no. 9, pp. 2295-2305, Sept. 2021, doi: 10.1109/TMI.2021.3076810.
- [7] Z. Chen et al., "High Temporal Resolution Total-Body Dynamic PET Imaging Based on Pixel-Level Time-Activity Curve Correction," in *IEEE Transactions on Biomedical Engineering*, vol. 69, no. 12, pp. 3689-3702, Dec. 2022, doi: 10.1109/TBME.2022.3176097.
- [8] G. Wang, W. Li, J. Du, B. Xiao and X. Gao, "Medical Image Fusion and Denoising Algorithm Based on a Decomposition Model of Hybrid Variation-Sparse Representation," in *IEEE Journal of Biomedical and Health Informatics*, vol. 26, no. 11, pp. 5584-5595, Nov. 2022, doi: 10.1109/JBHI.2022.3196710.
- [9] Y. A. Bayhaqi, A. Hamidi, F. Canbaz, A. A. Navarini, P. C. Cattin and A. Zam, "Deep-Learning-Based Fast Optical Coherence Tomography (OCT) Image Denoising for Smart Laser Osteotomy," in *IEEE Transactions on Medical Imaging*, vol. 41, no. 10, pp. 2615-2628, Oct. 2022, doi: 10.1109/TMI.2022.3168793.
- [10] J. Xu, X. Deng and M. Xu, "Revisiting Convolutional Sparse Coding for Image Denoising: From a Multi-Scale Perspective," in *IEEE Signal Processing Letters*, vol. 29, pp. 1202-1206, 2022, doi: 10.1109/LSP.2022.3175096.
- [11] H. Liu et al., "PET Image Denoising Using a Deep-Learning Method for Extremely Obese Patients," in *IEEE Transactions on Radiation and Plasma Medical Sciences*, vol. 6, no. 7, pp. 766-770, Sept. 2022, doi: 10.1109/TRPMS.2021.3131999.
- [12] Y. Cao et al., "Remote Sensing Image Recovery and Enhancement by Joint Blind Denoising and Dehazing," in *IEEE Journal of Selected Topics in Applied Earth Observations and Remote Sensing*, vol. 16, pp. 2963-2976, 2023, doi: 10.1109/JSTARS.2023.3255837.
- [13] D. Wu, H. Ren and Q. Li, "Self-Supervised Dynamic CT Perfusion Image Denoising With Deep Neural Networks," in *IEEE Transactions on Radiation and Plasma Medical Sciences*, vol. 5, no. 3, pp. 350-361, May 2021, doi: 10.1109/TRPMS.2020.2996566.
- [14] Y. Cheng et al., "Pasadena: Perceptually Aware and Stealthy Adversarial Denoise Attack," in *IEEE Transactions on Multimedia*, vol. 24, pp. 3807-3822, 2022, doi: 10.1109/TMM.2021.3108009.
- [15] Y. Wang, X. Song and K. Chen, "Channel and Space Attention Neural Network for Image Denoising," in *IEEE Signal Processing Letters*, vol. 28, pp. 424-428, 2021, doi: 10.1109/LSP.2021.3057544.
- [16] S. G. Bahnemiri, M. Ponomarenko and K. Egiazarian, "Learning-Based Noise Component Map Estimation for Image Denoising," in *IEEE Signal Processing Letters*, vol. 29, pp. 1407-1411, 2022, doi: 10.1109/LSP.2022.3169706.
- [17] Y. -C. Miao, X. -L. Zhao, X. Fu, J. -L. Wang and Y. -B. Zheng, "Hyperspectral Denoising Using Unsupervised Disentangled Spatospectral Deep Priors," in *IEEE Transactions on Geoscience and Remote Sensing*, vol. 60, pp. 1-16, 2022, Art no. 5513916, doi: 10.1109/TGRS.2021.3106380.
- [18] D. Zhang and F. Zhou, "Self-Supervised Image Denoising for Real-World Images With Context-Aware Transformer," in *IEEE Access*, vol. 11, pp. 14340-14349, 2023, doi: 10.1109/ACCESS.2023.3243829.
- [19] H. Liu, J. Zhang and R. Xiong, "CAS: Correlation Adaptive Sparse Modeling for Image Denoising," in *IEEE Transactions on Computational Imaging*, vol. 7, pp. 638-647, 2021, doi: 10.1109/TCI.2021.3083135.
- [20] H. Yin and S. Ma, "CSformer: Cross-Scale Features Fusion Based Transformer for Image Denoising," in *IEEE Signal Processing Letters*, vol. 29, pp. 1809-1813, 2022, doi: 10.1109/LSP.2022.3199145.
- [21] H. Liu, L. Li, J. Lu and S. Tan, "Group Sparsity Mixture Model and Its Application on Image Denoising," in *IEEE Transactions on Image Processing*, vol. 31, pp. 5677-5690, 2022, doi: 10.1109/TIP.2022.3193754.
- [22] K. Chen, X. Pu, Y. Ren, H. Qiu, F. Lin and S. Zhang, "TEMNet: A Novel Deep Denoising Network for Transient Electromagnetic Signal With Signal-to-Image Transformation," in *IEEE Transactions on Geoscience and Remote Sensing*, vol. 60, pp. 1-18, 2022, Art no. 5900318, doi: 10.1109/TGRS.2020.3034752.
- [23] Ulu, G. Yildiz and B. Dizdaroğlu, "MLFAN: Multilevel Feature Attention Network With Texture Prior for Image Denoising," in *IEEE*

- Access, vol. 11, pp. 34260-34273, 2023, doi: 10.1109/ACCESS.2023.3264604.
- [24] J. -J. Huang and P. L. Dragotti, "WINNet: Wavelet-Inspired Invertible Network for Image Denoising," in *IEEE Transactions on Image Processing*, vol. 31, pp. 4377-4392, 2022, doi: 10.1109/TIP.2022.3184845.
- [25] S. Su et al., "Accelerated 3D bSSFP Using a Modified Wave-CAIPI Technique With Truncated Wave Gradients," in *IEEE Transactions on Medical Imaging*, vol. 40, no. 1, pp. 48-58, Jan. 2021, doi: 10.1109/TMI.2020.3021737.
- [26] Y. Hel-Or and G. Ben-Artzi, "The Role of Redundant Bases and Shrinkage Functions in Image Denoising," in *IEEE Transactions on Image Processing*, vol. 30, pp. 3778-3792, 2021, doi: 10.1109/TIP.2021.3065226.
- [27] W. Zhu, X. Ma, X. -H. Zhu, K. Ugurbil, W. Chen and X. Wu, "Denoise Functional Magnetic Resonance Imaging With Random Matrix Theory Based Principal Component Analysis," in *IEEE Transactions on Biomedical Engineering*, vol. 69, no. 11, pp. 3377-3388, Nov. 2022, doi: 10.1109/TBME.2022.3168592.
- [28] K. Lee and W. -K. Jeong, "ISCL: Interdependent Self-Cooperative Learning for Unpaired Image Denoising," in *IEEE Transactions on Medical Imaging*, vol. 40, no. 11, pp. 3238-3248, Nov. 2021, doi: 10.1109/TMI.2021.3096142.
- [29] H. Sun, M. Liu, K. Zheng, D. Yang, J. Li and L. Gao, "Hyperspectral Image Denoising via Low-Rank Representation and CNN Denoiser," in *IEEE Journal of Selected Topics in Applied Earth Observations and Remote Sensing*, vol. 15, pp. 716-728, 2022, doi: 10.1109/JSTARS.2021.3138564.
- [30] X. Tian, F. He, R. Liu and J. Ma, "Interpretable Poisson Optimization-Inspired Deep Network for Single-Photon Counting Image Denoising," in *IEEE Transactions on Instrumentation and Measurement*, vol. 72, pp. 1-11, 2023, Art no. 5002111, doi: 10.1109/TIM.2022.3228266.
- [31] Sivakumar, R. & Balaji, G. & Ravikiran, R.S.J. & Ramasamy, Karikalan & Janaki, S.. (2009). Image Denoising using Contourlet Transform. *Computer and Electrical Engineering*, International Conference on. 1. 22-25. 10.1109/ICCEE.2009.70.
- [32] Meneses-Claudio, B. ., Perez-Siguas, R. ., Matta-Solis, H. ., Matta-Solis, E. ., Matta-Perez, H. ., Cruzata-Martinez, A. ., Saberbein-Muñoz, J. ., & Salinas-Cruz, M. . (2023). Automatic System for Detecting Pathologies in the Respiratory System for the Care of Patients with Bronchial Asthma Visualized by Computerized Radiography. *International Journal on Recent and Innovation Trends in Computing and Communication*, 11(2), 27-34. <https://doi.org/10.17762/ijritcc.v11i2.6107>
- [33] Jones, D., Taylor, M., García, L., Rodriguez, A., & Fernández, C. Using Machine Learning to Improve Student Performance in Engineering Programs. *Kuwait Journal of Machine Learning*, 1(1). Retrieved from <http://kuwaitjournals.com/index.php/kjml/article/view/101>